Glider Observations of Optical Backscatter in Different Jerlov Water Types: Implications to US Naval Operations

K. L. Mahoney and N. D. Allen
Naval Oceanographic Office
1002 Balch Blvd.
Stennis Space Center, MS 39522 USA

Abstract- **Unmanned underwater vehicles (UUVs) are increasingly being used as efficient and cost-effective Intelligent Preparation of the Operational Environment (IPOE) platforms by the Naval Oceanographic Office (NAVOCEANO), which seeks to provide Battlespace on Demand to the US Navy warfighter. One such UUV, the Teledyne/Webb Slocum Electric Glider, was utilized during four US Naval exercises in the past year to provide environmental data in support of Navy operations. Folding Slocum Glider missions into tactical operations has numerous benefits: the Slocum Glider (1) provides high-resolution optical and physical data in shallow coastal environments in real-time, (2) maintains a low profile when surfaced, (3) is piloted remotely with minimal manpower, (4) can be deployed over-the-horizon, and (5) reduces the amount of time an asset spends off-mission for the sake of IPOE measurements. Environmental data include sound velocity profiles, water clarity, and current velocity. The scientific payload for the Slocum Gliders in the NAVOCEANO glider inventory consists of a CTD probe and an optical backscattering sensor. Sound velocity profiles are derived from the CTD, water clarity is inferred from the backscattering data, and depth-averaged currents are determined by offsets between subsurface dead-reckoning position estimates and actual surface Global Positioning System (GPS) position fixes. One issue pertaining to the optical data is that many of the optical products utilized are based on beam attenuation and not optical backscattering. Consequently, optical backscattering data from the NAVOCEANO Slocum glider data must be converted to beam attenuation to be utilized for algorithms that create optical products. The work presented here examines the optical backscattering to beam attenuation relationship of glider-based observations of four distinct coastal water masses, as described by the Jerlov Optical Ocean Water Mass Classification. Optical backscattering data were converted to beam attenuation by (1) using a standard algorithm and (2) scaling backscattering to attenuation. The results indicate that the contribution of optical backscatter to total attenuation depends heavily on the composition of particles in the water column and that concurrent measures of beam attenuation and optical backscattering are needed to provide accurate estimates of relevant optical products.**

I. INTRODUCTION

The Naval Oceanographic Office (NAVOCEANO) recently added unmanned underwater vehicles (UUVs), specifically gliders, to its repertoire of ocean sensing capabilities. Gliders are capable of providing high-resolution oceanographic and Intelligent Preparation of the Operational Environment (IPOE) data with minimal manpower. Further, the unit cost of a glider is equivalent to the cost of two days ship time, and a glider can remain deployed for up to 180 days, depending upon the type of glider used. NAVOCEANO's operational use of gliders began during the summer of 2007, when four Sea-gliders (developed by the University of Washington Applied Physics Lab) were deployed in support of a Navy exercise near Guam [1]. By July 2008, NAVOCEANO's glider inventory had grown to eight Sea-gliders and two Slocum Electric Gliders (Teledyne/Webb), and NAVOCEANO's Glider Operation Center (GOC) simultaneously piloted multiple Sea-gliders and Slocum gliders in support of a Navy exercise near the Hawaiian Islands [2]. NAVOCEANO's inventory of Sea-gliders and Slocum gliders continues to increase as does the demand for glider support by the Fleet. During FY09, Slocum gliders were used in four naval exercises and one Maritime Homeland Defense exercise.

The IPOE data pertinent to naval operations include sound velocity profiles, water clarity, and current vectors. Operational demonstrations have shown that Slocum glider-based data are useful for electro-optical identification (EOID) sensor performance prediction [3] and for tuning sonar systems during operations, thereby maximizing the efficient use of assets and minimizing the risks involved when using vessel-borne measurement systems. At present, the scientific payload for the Slocum Gliders in the NAVOCEANO glider inventory consists of commercially available Conductivity, Temperature, and Depth (CTD) probes and optical backscattering sensors. These scientific payloads are capable of detecting subtle changes in the optical and physical parameters of the water column. Sound velocity profiles are derived from the CTD, water clarity is inferred from the optical backscattering data, and depth-averaged currents are determined by offsets between subsurface dead-reckoning position estimates and actual surface Global Positioning System (GPS) position fixes.

Many generic optical products, such as diver visibility or light detection and ranging (LIDAR) beam penetration range, are derived from beam attenuation [4, 5, 6]. Beam attenuation differs from optical backscatter in that beam attenuation describes the loss of light due to both absorption and scattering as the light travels between two points whereas optical backscattering is the portion of scattering that is in the opposite direction to that of the light propagation, and it is dependent upon particle composition,

0-933957-38-1 ©2009 MTS

shape, and particle size distribution. The work presented here examines the relationship between optical backscattering and beam attenuation via glider-based observations of four distinct coastal water masses. Each water mass that was used for this comparison corresponds to a different water type of the Jerlov Optical Ocean Water Mass Classification [7, 8]. As the optical constituents among the different water types will vary, the contribution of scattering, and therefore backscattering, to total attenuation is expected to vary as well. The goal of this work is to determine the most appropriate way to convert backscattering to attenuation in order to maximize the optical backscattering data on the Slocum glider.

II. Methods and Materials

Both attenuation and backscattering are wavelength dependent, and this paper focuses solely on 532 nm wavelength for both optical parameters. Profiles of optical backscattering from Slocum glider missions in four different water masses were analyzed. The oligotrophic waters southeast of Oahu, Hawaii represented Type I water mass (clear oceanic water) and had the lowest optical backscattering of the four water types (Fig. 1).

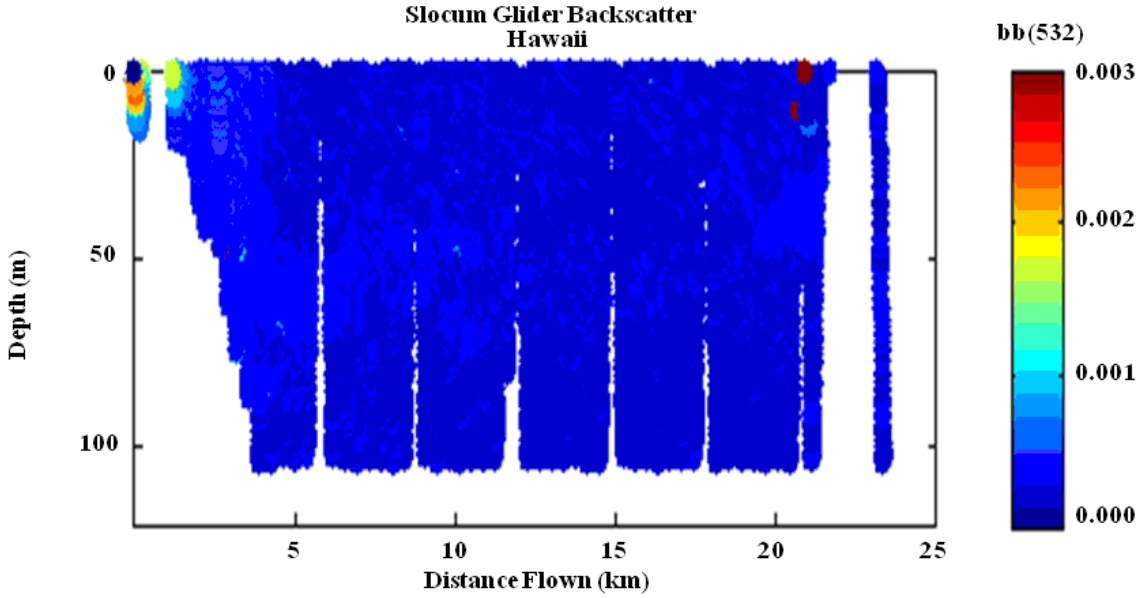

Fig. 1 Optical backscatter (bb(532)) measured with a bb3slo onboard a Slocum in Hawaiian waters. The color bar shows the magnitude of backscatter for each profile. The Hawaiian waters were the clearest of the waters examined.

Waters in the Ligurian Sea represented transitional Type Ia (clear coastal water with higher attenuation than Type I) and II waters (turbid coastal water) (Fig. 2).

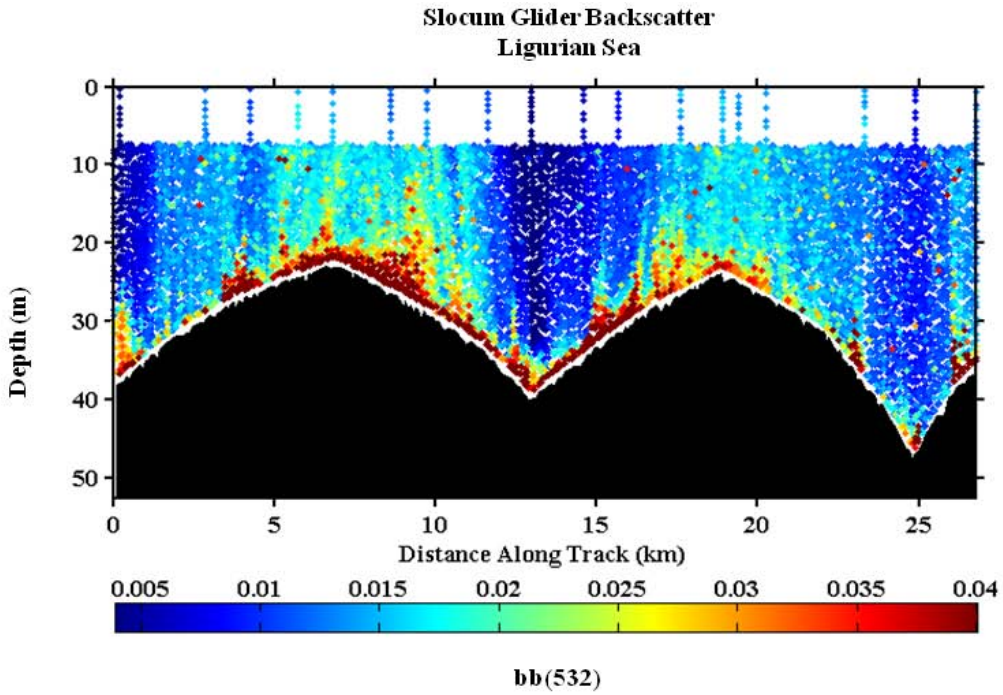

Fig. 2 Optical backscatter (bb(532)) from the bb3slo aboard a Slocum operating in the Ligurian Sea. These waters ranged from clear to turbid, depending upon depth and proximity to coast. Inorganic material dominated the shallow waters, and organic material was the dominant constituent of the deeper waters. The magnitude of backscatter is shown in the color bar.

Waters in the Arabian Gulf, dominated by aeolian dust input, were representative of Type Ib water (more turbid coastal waters than Type I) (Fig. 3).

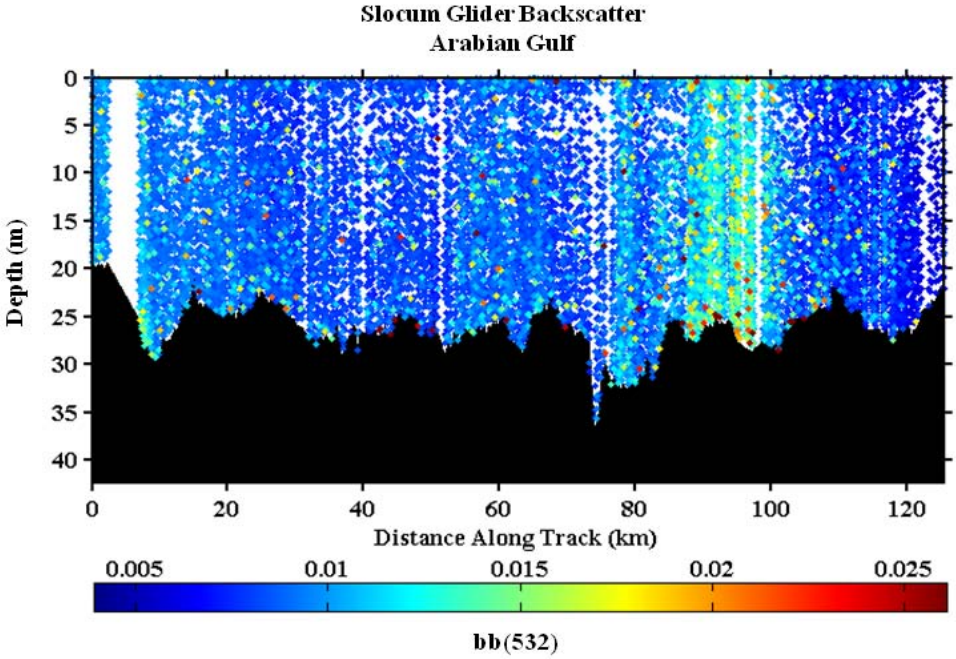

Fig. 3 Optical backscatter (bb(532)) from the bb3slo aboard a Slocum operating in Arabian Gulf waters. Shamals (dust storms) contributed to the optical properties of this area, and it is assumed that inorganic material is the predominant optical constituent of this area. The magnitude of backscatter is shown in the color bar.

The area of the Yellow Sea that was examined is dominated by eutrophication from anthropogenic input and suspended sediments, and these waters represent Type III water (murky coastal water) and had the highest backscattering values of the four water types (Fig. 4).

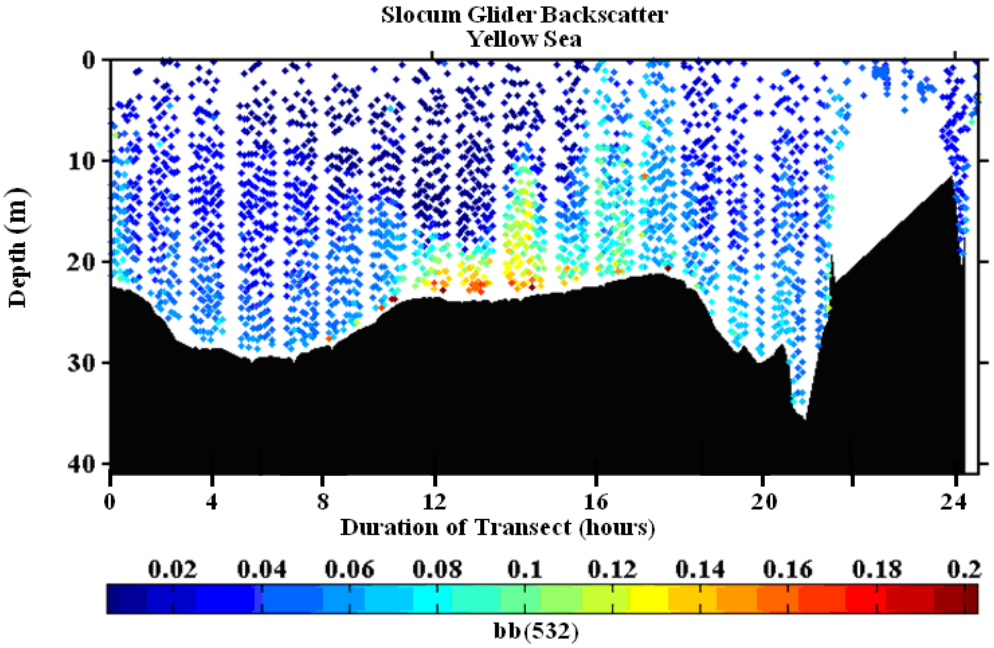

Fig. 4 Optical backscatter (bb(532)) from the bb3slo aboard a Slocum in the Yellow Sea. These waters were the most turbid of the waters, and it is assumed for this area that organics and inorganics are equal optical constituents.

The backscattering data measured in the four different water types were converted to beam attenuation using three different methods. The first method assumes a uniform particle composition in the water column, an average backscattering to total scattering ratio of 0.01 [9], and an average albedo of 0.8 [10]. Using this method, the scaling factor to convert backscatter (b_b) into attenuation (c) is 125 for natural waters [11] such that

$$c = 125 * b_b. \quad (1)$$

The second method uses the linear relationship between beam attenuation and backscattering in order to calculate beam attenuation from backscatter. Seven data sets from inner coastal to very clear open ocean—with approximately 7000 1-m bins and approximately 300,000 individual measurements of beam attenuation and concurrent backscattering—were plotted against each other [12], and the linear fit of the data was described by the equation

$$c = 69.5*b_b + 0.073. \quad (2)$$

The third method cross-references in situ measures of backscattering to in situ measures of beam attenuation to derive a scaling factor. Assuming a consistent particle composition for the local area throughout the Slocum mission, one can obtain a scaling factor by dividing the beam attenuation by optical backscattering. The scaling factor (SF) could then be applied to the subsequent backscattering data to make the conversion to attenuation as in

$$c = SF * b_b. \quad (3)$$

To obtain the scaling factor in (3) for the Hawaiian waters, the measured backscattering was cross-referenced with beam attenuation measured by a Wet Labs, Inc. AUV-b, which was in the science payload of two of the four Slocum gliders deployed for the Hawaiian exercise. The other two gliders had bb3slo's in their scientific payload. For the Yellow Sea and the Arabian Gulf, the initial measured backscattering was cross-referenced with beam attenuation values measured with a Wet Labs C-star transmissometer at the onset of the glider mission. For the Ligurian Sea, backscattering data were cross-referenced to beam attenuation measured with a Wet Labs, Inc. DOLPHIN (i.e., an optical towed body) at the same time and location as the start of the Slocum mission. The DOLPHIN was also in the vicinity of the Slocum glider at the 20 m isobath and observed the same turbid waters as the glider. Having beam attenuation data for the 40 m isobath and the 20 m isobath allowed two cross-references to the backscattering data, and consequently, the Ligurian Sea is broken into Type Ia and Type II water masses.

III. Results and Discussion

Table I provides a summary of the results obtained in converting optical backscatter into attenuation. For each area, the average backscattering data for the first Slocum profile is shown, as is the average attenuation data for the same area and time.

TABLE I
DIFFERENT CONVERSIONS OF BACKSCATTER TO ATTENUATION

Area	Avg. Backscatter	Avg. Attenuation	Calculated c	Calculated c	Scaling Factor	Initial c
	(m^{-1})	(m^{-1})	$c = 125*b_b$	$c = 69.5*b_b + 0.073$	In situ cross ref.	In situ cross ref.
Hawaii (Type I)	0.0008	0.096	0.1	0.123	$120 * b_b$	0.096
Ligurian Sea (Type Ia)	0.004	0.4	0.5	0.351	$100 * b_b$	0.4
Ligurian Sea (Type II)	0.04	1.5	5.0	2.85	$37.5 * b_b$	1.5
Arabian Gulf (Type Ib)	0.008	1.05	1.25	0.768	$105* b_b$	1.05
Yellow Sea (Type III)	0.04	5.6	5.0	2.85	$140 * b_b$	5.6

The fourth and fifth columns show the resulting attenuation value (m^{-1}) obtained by using (1) and (2), respectively. The sixth column provides the scaling factor for each area obtained by dividing the average measured backscatter into the average attenuation, and the seventh column shows the attenuation by using (3).

Aside from the third column and seventh columns being equal—which was expected—no clear trend emerges for the data in Table I. Similar results were obtained with (1) and (2) for the Type I, Type Ia, and Type Ib waters when compared to the measured value of the same area. Equation (1) had a tendency to overestimate the calculated beam attenuation, except for the Type III water mass, and (2) underestimated the calculated beam attenuation for the different water types, except for the Type I water mass.

Table II shows the range of values for beam attenuation if (1), (2), and (3) are applied to the entire range of the backscattering values observed by the Slocum gliders in the different water types.

TABLE II
RANGE OF ATTENUATION VALUES DERIVED FROM THE RANGE OF OBSERVED BACKSCATTERING VALUES

Area	Range of b_b	Range of c (1)	Range of c (2)	Range of c (3)	Actual Range of c
	(m^{-1})	(m^{-1})	(m^{-1})	(m^{-1})	(m^{-1})
Hawaii (Type I)	0.0008 – 0.0012	0.1– 0.15	0.123 – 0.1564	0.096 – 0.144	0.09 – 0.16
Ligurian Sea (Type Ia)	0.004 – 0.02	0.5 – 2.5	0.351 – 1.463	0.4 – 2.0	0.15 – 0.7
Ligurian Sea (Type II)	0.02 – 0.04	2.5 – 5	1.463 – 2.85	0.75 – 1.5	0.7 – 1.5
Arabian Gulf (Type Ib)	0.008 – 0.025	1.25 – 3.25	0.768 – 1.81	0.768 – 0.938	N/A
Yellow Sea (Type III)	0.04 – 0.2	5.0 – 25.0	5.0 – 13.93	5.6 – 28.0	N/A

Beam attenuation data were available for the entire Slocum missions in Hawaii and the Ligurian Sea (Fig. 5); however, attenuation data existed only for the start of the Slocum missions in the Yellow Sea and the Arabian Gulf. The range of attenuation values calculated for Hawaii using the three conversion methods was in agreement with the observed attenuation values for the area. All three methods overestimated the range of attenuation values for the Type I waters; however, the method of cross-referencing the measured backscattering data to measured attenuation data to derive the scaling factor was in agreement with the observed values. The agreement of this method to the observed results for this one area does not necessarily suggest that this method is the preferred method for converting backscatter to attenuation. Given that optical properties are highly variable on small spatial and temporal scales, the optical constituents should also be considered highly variable on small spatial and temporal scales. Along with this variability in constituents comes variability in the proportion of backscattering to total scattering ratio and the total scattering to attenuation ratio. Such variability changes with the particulate size distribution and particulate composition in the water column, which explains the different magnitudes of backscattering for the different water types as well as the various ranges seen in the derived data.

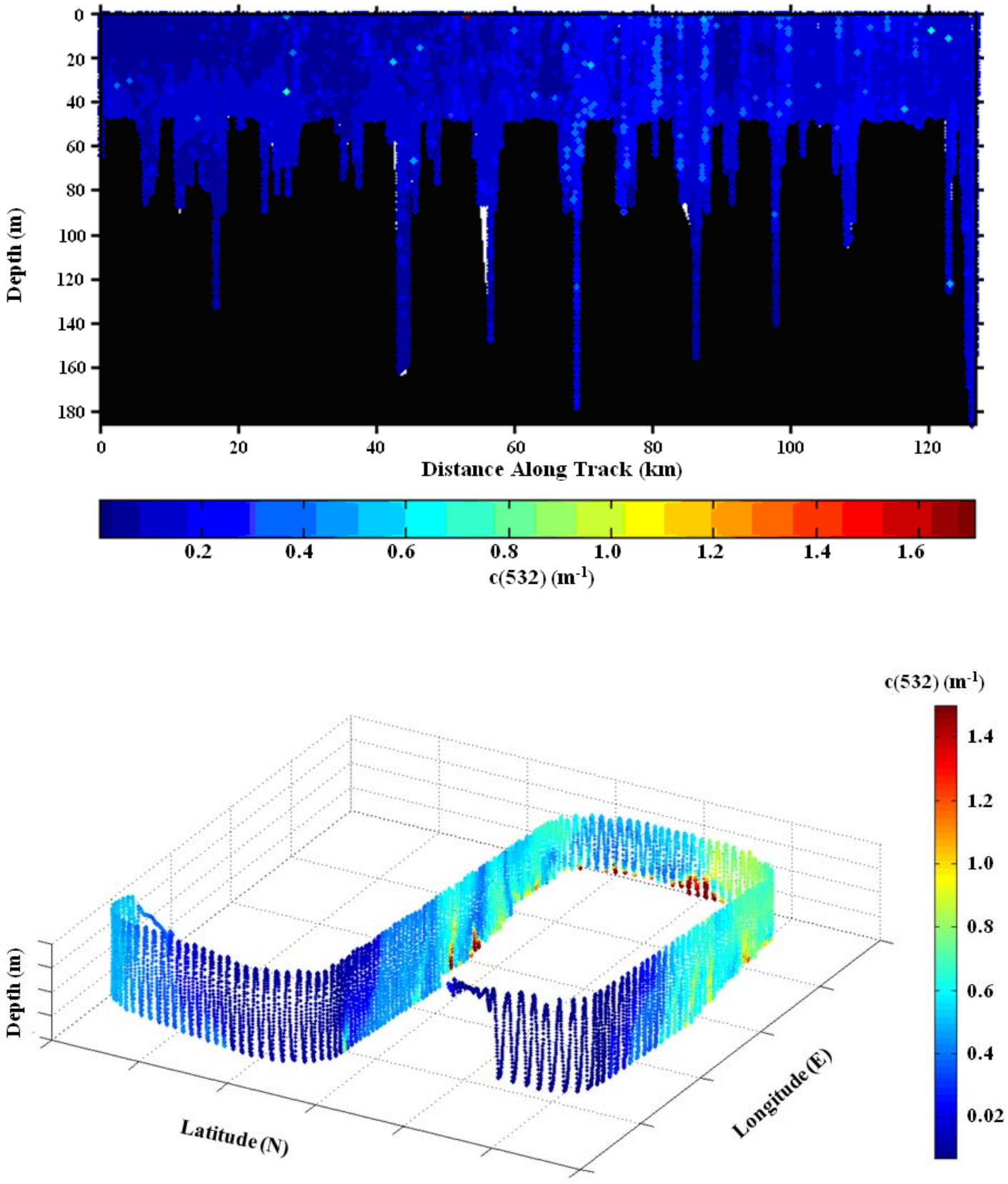

Fig. 5 Beam attenuation values measured with the AUV-b on the Slocum glider for Hawaii (top) and measured with the DOLPHIN in the Ligurian Sea (bottom) during the Slocum missions in the area. DOLPHIN image courtesy of Mike Twardowski.

The outstanding question is how these data will affect products generated for the US Navy. Table III shows diver visibility and EOID detection limits based on derived beam attenuation data for each method.

TABLE III
OPTICAL PRODUCTS BASED ON DERIVED ATTENUATION VALUES

Area	Diver Visibility (1)	Diver Visibility (2)	Diver Visibility (3)	LIDAR range (1)	LIDAR range (2)	LIDAR range (3)
	(m)	(m)	(m)	(m)	(m)	(m)
Hawaii (Type I)	48	40	50	30	24	31
Ligurian Sea (Type Ia)	9.6	13.7	12	6	8.5	7.5
Ligurian Sea (Type II)	0.96	1.7	3.2	0.6	1.05	2.0
Arabian Gulf (Type Ib)	3.84	6.25	4.57	2.4	3.9	2.8
Yellow Sea (Type III)	0.96	1.7	0.87	0.6	1.05	0.53

Diver visibility was calculated with beam attenuation as in [4], and a generic LIDAR beam penetration range for object detection was calculated using three attenuation lengths [13]. The number in parenthesis next to each product represents the equation used for the derivation. The end result for each product in each water type is essentially the same. If an operational planner wanted to know good, marginal, or bad optical conditions, then the resulting products were the same for all water types. In short, each method provided variable estimates of beam attenuation for each water type, but the variability is not reflected in the products and is therefore inconsequential to the warfighter.

IV. CONCLUSION

The goal of this work was to understand the efficiency of using solely optical backscatter data for optical products in support of the US Navy. Optical backscattering data from Slocum glider missions in different Jerlov water types were converted to beam attenuation using three simplistic methods. Variability existed in the resulting attenuation estimates from the three methods, and agreement in the converted values to actual observations existed more so for the clear waters than the more complex turbid waters. It is recommended that ship-based optical measurements continue to be made at the onset of each glider mission, even though the assumption of consistent particle composition for local oceanic areas does not appear to be valid. As to which algorithm works best in converting backscattering to beam attenuation data, while there is significance from a scientific standpoint, the results suggest that the answer is operationally irrelevant to the warfighter.

ACKNOWLEDGMENT

The authors would like to thank the captains and crews of R/V ALLIANCE and numerous other ships for their hospitality and assistance while afloat. Additionally, the authors wish to thank Mr. John Kerfoot (Rutgers University), Dr. Mike Twardowski (Wet Labs, Inc.), Mr. Peter Collins (Teledyne/Webb), Mr. Ben Allsup (Teledyne/Webb), and Mr. Clayton Jones (Teledyne/Webb) for their support and assistance along the way. Finally, a special thanks to Mr. Ronald Betsch (MIW PM), Mr. Marc Torres (NAVOCEANO), the NAVOCEANO GOC pilots, and the Naval Oceanography Mine Warfare Center Reach Back Cell.

DISCLAIMER

The inclusion of names of any specific commercial product, commodity, or service in this paper is for information purposes only and does not imply endorsement by the US Navy or NAVOCEANO.

REFERENCES

[1] K. Mahoney, R. Arnone, P. Flynn, B. Casey, and S. Ladner, "Ocean Optical Forecasting in Support of MCM Operations," Proc. of 8th Int. MINWARA Conference of Technology and the Mine Problem, 2008.

[2] K. Mahoney, K. Grembowicz, B. Bricker, S. Crossland, D. Bryant, M. Torres, and T. Giddings, "RIMPAC 08: Naval Oceanographic Office Glider Operations," *Proc. of SPIE*, vol. 7317, 731706, doi: 10.1117/12.820492, 2009.

[3] K. Mahoney, O. Schofield, J. Kerfoot, T. Giddings, J. Shirron, and M. Twardowski, "Laser Line Scan Performance Prediction," *Proc. of* SPIE, vol. 6675, 66750N, doi: 10.1117/12.7344617, 2007.

[4] J. Zaneveld and W. Pegau, "Robust Underwater Visibility Parameter," Optics Express, vol. 11 (23), pp 2997 – 3009, 2003.

[5] R. Vollmerhausen, "Modelling the Performance of Imaging Sensors," *Electro-optical Imaging: Systems and Modeling*, Chapter 12, ed. L. Biberman, pp. 1220, SPIE Press (Bellingham, WA), 2000.

[6] T. Giddings, J. Shirron, and A. Tirat-Gefen, "EODES-3: An Electro-optic Imaging and Performance Prediction Model," *MTS/IEEE Oceans 2005 Conf. Proc.*, vol. 2, pp. 1380 -1387, 2005.

[7] N. Jerlov, “Optical Classification of Ocean Water,” In: Physical Aspects of Light in the Sea, Univ. of Hawaii Press, Honolulu, Hawaii, pp. 45 – 49, 1964.
[8] N. Jerlov, *Optical Oceanography*, Elsevier Pub., New York, pp. 194, 1968.
[9] J. Sullivan and M. Twardowski, unpublished.
[10] A. Barnard, W. Pegau, and J. Zaneveld, “Global Relationships in the Inherent Optical Properties of the Oceans,” *J. Geophys. Res*., vol. 103, 24,955 – 24,968, 1998.
[11] M. Twardowski, unpublished.
[12] M. Twardowski et al., unpublished.
[13] J. Jaffe, “Underwater Optical Imaging: the Design of Optimal Systems,” *Oceanography*, November, 1988.